STUDIES OF THE MECHANICAL BEHAVIOR OF AMMONIUM PERCHLORATE PARTICLES, A GLASS-BEAD FILLED POLYURETHANE BINDER, AND A TYPICAL CONTINUUM BINDER

P. J. Blatz

Firestone Flight Sciences Laboratory
Graduate Aeronautical Laboratories
California Institute of Technology
Pasadena, California

ABSTRACT

Experimental studies were carried out on a continuum Neoprene binder, a glass bead-filled-polyurethane binder, and unbound micro-pulverized ammonium perchlorate particles. As a result of stress relaxation and creep experiments, it is concluded that the large deformation behavior of the filled binder can be described in part in terms of the large deformation behavior of the continuum binder. The time scale of relaxation of stress in the filled binder is much longer than that of the unfilled binder. It is determined by frictional processes between the filler and binder and also among the filler particles.

As a result of relaxation and creep studies on ammonium perchlorate particles, it is found that the time scale of relaxation is of the same order of magnitude as that of the filled binder. In addition, it is believed that the static indeterminacy of the unbound particles helps to explain much of the strain variation at given stress level that is observed in tensile experiments of composite propellants.

I. INTRODUCTION

This memo presents an interim report of some of the studies being conducted at GALCIT on the mechanical properties of composite propellants. Because of the radically new approach to an understanding of these properties which is presented below, the writer will first recall some of the historic facts associated with the evolution of our present day knowledge of composite propellants. Then will follow a discussion of studies carried out during the last six months. Finally, a statement of outstanding problems and projected future studies will be cast forth.

II. CHRONOLOGY

After the discovery at Jet Propulsion Laboratory (1948) of "liquid polymers," rubber-base propellants became a reality. It took six years (1954) to develop really useful rubber composites based on polyurethane, and polysulfide binders, and three more years (1957) to bring polybutadiene binders into the picture. All of these materials helped revolutionize the design of rocket motors. The era of large rocket motors (diam. > 30 in.) opened up when binders could accommodate >20% thermal strain.

Because of the importance of these binders, all rocket companies initiated broad research programs on their physical and mechanical properties.

In 1954, the writer, then an employee of the Aerojet-General Corporation, initiated a series of studies (1) on polyurethane composites which brought to light some of the most important features of this system. These are summarized below without harking back to the details which lead to these conclusions.

1. The first response of a polyurethane composite to any stress field is elastic deformation with no attendant volume change.

2. At some point in the deformation process, more or less well defined, the binder pulls away from the filler particles, with attendant volume increase.

3. The point at which this pullaway initiates may be markedly altered by the absence or presence of special additives which promote adhesion between the binder and the filler. In complete absence of such adhesives, the point of pullaway is blurred; and it may actually occur over a broad range of strain. Thus pullaway is associated with a distribution of adhesion strengths. If the adhesion strength is weaker than the binder strength, the binder will pull away causing the composite to tear at some weak point. This will usually propagate locally and lead to the so-called "zebra-stripe" type of local failure. If the adhesion strength is stronger than the binder strength, the binder will yield (highly-filled composites are not well cured) and will hang onto the particles. This will make for much higher ultimate strains at slightly lower ultimate stress levels than in the absence of the adhesive.

4. Poisson's ratio, properly defined (cf. below) falls off to a value of 1/4 as pullaway goes to completion.

5. If the deformation process is interrupted and relaxation of stress allowed to occur, it is found that the filler particles are driven by local stress concentrations in the binder and move slowly to new positions of equilibrium and retarded by binder-particle frictional forces.

6. If the relaxation process is allowed to ensue indefinitely at a given strain level, a propellant sample will eventually fail providing a minimum critical strain of about 30% in simple tension is exceeded. Below this critical strain, the propellant sample will not fail but the original stress will relax to a few tenths of a psi. After removal of the given fixed strain, the sample will recover completely. It follows that, if a propellant sample is held at a fixed stress in excess of a few tenths of a psi, failure will ensue.

These observations raise a number of questions: What is the time scale associated with the frictional forces? How important are interparticle frictional forces as compared to binder-particle frictional forces? What is the meaning of the high critical strain relative to the low critical stress level?

As a result of a number of growing convictions that arise out of these and later studies, (2, 3, 4) the writer believes that the final understanding of the mechanical behavior of composite propellants must come out of separate studies on idealized systems:

1. The continuum binder.
2. The unfilled foamed binder.
3. The filled but completely dewetted binder.
4. The filled binder in some defined state of adhesion to filler.
5. The unbound filler (a granular medium).

Each of these systems is discussed below, in the course of which some of the answers to the previously posed questions will be provided.

III. CONTINUUM BINDERS

Much is and has been known, of course, about the mechanical behavior of continuum rubbers. (5) In addition, a three year study program (6) in GALCIT has provided additional information regarding failure properties of continuum rubbers. The complete response behavior of a continuum rubber is contained in the strain energy density (W) which, because of the principle of material indifference to rigid body motions in isotropic space, is an explicit function of the stretch invariants:

$$J_1 = \Sigma \lambda_i^2 \tag{1}$$

$$J_2 = \Sigma \frac{1}{\lambda_i}^2 \tag{2}$$

$$\frac{V}{V_0} = J_3 = \pi \lambda_i \tag{3}$$

where λ_i = stretch ratio along a principal geometric axis; i = 1, 2, 3. The constitutive equation derived from W by the principle of virtual work is given by:

$$\bar{\sigma}_1 J_3 = \sigma_i \lambda_i = 2\left[W_1 \lambda_i^2 - \frac{W_2}{\lambda_i^2}\right] + J_3 W_3 \tag{4}$$

where $\bar{\sigma}_i$ = true stress

σ_i = engineering stress or load/undeformed area

$W_k \equiv \frac{\partial W}{\partial J_k}$

For most rubberlike materials, W_1 and W_2 may be treated as constants, in which case we write:

$$W_1 = \frac{\mu}{2}(f) \tag{5}$$

$$W_2 = \frac{\mu}{2}(1-f) \tag{6}$$

$$W_1 + W_2 = \frac{\mu}{2} \text{ in agreement with Hooke's Law} \tag{7}$$

$$W_{13} = W_{23} = 0 \tag{8}$$

$$W_3 = W_3 \ (J_3 \text{ only}) \tag{9}$$

Furthermore, most continuum rubbers are practically incompressible, in which case (4) becomes:

$$\overline{\sigma_i} = \sigma_i \lambda_i = \mu \left[f \lambda_i^2 - \frac{1-f}{\lambda_i^2} \right] + \overline{k};\ J_3 = 1 \tag{10}$$

where $\overline{k}$ is a parameter which depends linearly on the hydrostatic stress.

For the special case of simple tension ($\lambda_1 = \lambda$; $\lambda_2 = \lambda_3 = 1/\sqrt{\lambda}$) to which we shall now restrict the discussion, (10) becomes:

$$\mu_{n\ell} \equiv \frac{\sigma}{\lambda - \frac{1}{\lambda^2}} = \mu \left[f + \frac{1-f}{\lambda} \right] \tag{11}$$

where $\mu_{n\ell}$ stands for non-linear shear modulus. Equation (11) suggests that a plot of $\mu_{n\ell}$ vs. $1/\lambda$ should yield a straight line if (5) and (6) are valid.

Figures 1, 2 and 3 show the form such plots take for data obtained on Neoprene - GNA Rubber* at + 75°F., 0°F., -75°F. In addition to the expected straight line region of each curve plotted at a given time and temperature, there is a region in Figures 1 and 2 beyond $\lambda = 3$, where the stress rises rapidly because of the onset of natural anisotropy. At the molecular level, this is due to the stretching of the chain to the limit of statistical extensibility. (7) Now it is noted that the slopes of the straight-line regions in Figures 1 and 3 remain constant, whereas, in the region of rapid up-sweep, the slope decreases rapidly with time until it is equal to the slope of the straight-line region. This implies that the chains are not well cured chemically and that, after they have been stretched out to the limit of their extensibility, either the chemical juncture points yield under stress or the entanglements slip. In either case, as time ensures, the character of the rubber becomes Mooney-Rivlin. Furthermore, since the slope remains constant with time, this implies that

$$\mu(1-f) = 2W_2 = \text{constant} \tag{12}$$

and therefore, since μ decreases with time, f and W_1 also decrease with time, and each becomes negative. Once they are negative, there is a maximum value of stretch which the network can sustain in tension, obtained by setting (11) equal to zero:

$$\lambda^* = 1 - \frac{1}{f} = - \frac{W_2}{W_1} \tag{13}$$

---

* Samples provided by courtesy of Dr. G. Kraus, Phillips Petroleum Corp.

It will be of interest to relate this value of λ^* to the ultimate or failure properties of the material.

Figure 4 shows how the shear modulus, obtained from the intercepts of the straight-line regions with the ordinates of Figures 1, 2 and 3 at $\lambda = 1$ varies with time at each of the three test temperatures. It is obvious that the 0° - 75°F. data fall well within the range of rubbery behavior, where the shear modulus is of the order of 100 psi, while the -75°F. data fall well within the range of glassy behavior, where the shear modulus is of the order of 100,000 psi, a thousandfold larger than the rubbery modulus.

The glass-transition temperature is estimated to be at -25°F., where future tests will be run. From these data will be obtained a complete quantitative characterization of the mechanical response of a typical binder. For the present, it can be said qualitatively that a typical binder in the rubbery temperature range behaves as a representative of a Mooney-Rivlin strain energy density with all the time dependence contained in the first Mooney-Rivlin constant.

This is a very important characterization for two reasons. First of all, it allows one to predict viscoelastic response to any kind of loading pattern-dynamic, quasi-static, which-have-you, by using the theory of non-linear viscoelasticity (8) which will be fully discussed in the next interim report.

In addition to the response behavior of a binder, it is important to characterize the failure behavior. In studies carried out in connection with a doctorate dissertation, (9) Ko has shown that the failure surface of natural rubber (2% sulfur) in the +++ octant of principal stress space is a tetrahedron, the three faces of which intersect at a right angle at an apex on the hydrostatic vector.

The projection of these three faces is of course the dilatational plane, so that the volume encompassed between the apex of the tetrahedron and the dilatational plane is 1/6 of a cube erected by mirrorlike reflection of the apex through each of the three coordinate planes. (cf. Figure 5) The physical significance of the failure criterion associated with this surface is that rupture occurs when the mean deviatoric stress reaches a critical value. Thus natural rubber does not fail by a dilatational mode, but does in fact exceed the critical values associated with the dilatational plane to fail by a distortional mode. This type of distortional mode may not be evinced in the ++- or +-- octants, in which case the failure surface would have to have convex discontinuities.

IV. FOAMED BINDERS

Although we have entered into a detailed discussion of the mechanical behavior of typical continuum rubbers in the previous discussion, we will only use this information to predict ab initio the mechanical behavior of foams in terms of the void content, hole size, and rubber phase properties. The equilibrium mechanical behavior of foams can be interpreted, independently of the previously mentioned factors, in terms of a strain-energy density which is associated with compressibility and a constitutive equation of the type (10).

Both of these points have been investigated. Ko (11) has shown that a polyurethane foam containing 47% voids is, for example, characterized by,

$$W_1 = 0 \tag{14}$$

$$W_2 = \frac{\mu}{2} \tag{15}$$

$$W_3 = \mu J_3^{\frac{4\nu-1}{1-2\nu}} \doteq \mu ; \quad \nu = 1/4 \tag{16}$$

Furthermore, he has been able to relate the measured value of $\nu (=1/4)$ to the void content of the foam, assuming the rubber phase to be incompressible. Thus a foamed rubber differs from a continuum rubber only in the form of the dilatation term: for the continuum rubber, k is a linear function of hydrostatic pressure; for the foam, J_3W_3 is a linear function of the dilatation, with $\nu = 1/4$. Both species of rubber are Mooney-Rivlinear in their shear behavior.

The equilibrium failure behavior of the polyurethane foam at 75°F. is quite simple. In the +++ octant, it occurs when the mean hydrostatic stress reaches a critical value. Thus the mode of failure is purely dilatational. It is not known where the distortional limit of failure occurs other than that it must occur in the ++- and +-- octants. Further studies under hydrostatic pressure are contemplated to determine the complete failure surface as well as its time and temperature dependence.

V. A FILLED BINDER

Like the unfilled foam, the filled binder dilates upon stretch and the constitutive equation (4) must be used to characterize it. In simple tension, this becomes, assuming Mooney-Rivlin shear behavior:

$$\sigma\lambda = \mu\left[f\lambda^2 - \frac{1-f}{\lambda^2}\right] + J_3W_3 \tag{17}$$

$$0 = \mu\left[f\frac{J_3}{\lambda} - \frac{(1-f)\lambda}{J_3}\right] + J_3W_3 \tag{18}$$

or equivalently,

$$\frac{\sigma}{\lambda - \frac{J_3}{\lambda^2}} \equiv \mu_{n\ell} = \mu\left[f + \frac{1-f}{\lambda J_3}\right] \tag{19}$$

$$\frac{W_3}{\mu} = \frac{(1-f)\lambda}{J_3^{\,2}} - \frac{f}{\lambda} \tag{20}$$

From a straight-line plot of $\mu_{n\ell}$ vs. $(1/\lambda J_3)$, one can determine μ and f. Equation (20) then allows one to calculate W_3 which can then be curvefitted to some function of J_3.

This procedure was carried out for data obtained in simple tension at 75°F. and 2 in./min. on a polyurethane binder filled with 70 vol. % glass beads. Figure 6 shows how the non-linear shear modulus varies with stretch ratio. Apparently there are two regions of behavior, one below 20% strain in which dewetting is complete. The reason for this latter conclusion becomes obvious when one looks at Figure 7, where the dilatational strain energy gradient is plotted vs. J_3. After $\lambda = 1.2$, the relation becomes linear. Within this range, one then has

$$\frac{W_3}{\mu} = A - BJ_3 \qquad (21)$$

Since this expression must reduce to Hooke's Law, A and B are uniquely determined in terms of Poisson's ratio leading to the expression:

$$\frac{W_3}{\mu} = \left[4(1-f) - \frac{2(1-\nu)}{1-2\nu}\right] - \left[2(1-\nu) - \frac{1}{1-2\nu}\right] J_3 \qquad (22)$$

Since A and B are interrelated, the calculation of ν serves as a double check on the self-consistency of the data and the assumption made in deriving (22). Both the measured slope and intercept of the straight-line region of Figure 7 give the same value of Poisson's ratio, e.g. $\nu = 1/4$. This is in striking agreement with the results obtained on unfilled foams. Thus a polyurethane propellant behaves after pullaway much like a foam.

The region in which pullaway occurs is the region in which f and μ fall off rapidly. After pullaway, f has become negative, so that we have the following comparison:

Neo-Hookean Continuum Rubber - $f = 1$, $\nu = 1/2$

Foamed Polyurethane Rubber
(50 Vol. % Holes) - $f = 0$, $\nu = 1/4$

Filled Polyurethane Rubber
(70 Vol. % Beads) - $f = -0.6$, $\nu = 1/4$
Pullaway at $\lambda = 1.2$

Before pullaway, f and μ must needs be strongly time and rate dependent. This phenomenon will be investigated in the immediate future.

In addition, a study of the relation between the above tabulated parameter and the state of adhesion of the binder to the beads is contemplated. For these studies, both Teflon and glass beads, along with various adhesives, will be used.

V. THE UNBOUND FILLER, OR GRANULAR MEDIUM

At room temperature, the average stress relaxation time for a continuum rubber held at a given stretch is of the order of nanoseconds. Anyone who has stretched a rubber band to a given stretch level is aware of the absence of any decrease in stress after arriving at the fixed stretch level. On the other hand, composite propellants do evince long-time stress relaxation in this sort of test. For example, a sample stretched

40% will take six months to relax its stress to less than 1% of the original value. Why this slow decay process? It is believed this is mostly due to particle-binder frictional forces, and partly to particle-particle frictional forces. Furthermore, it is believed that most binders filled with 80 - 90 wt. % of particles are not well cured, and that, during the six months of relaxation, the chains disentangle and yield. This picture is consistent with the behavior shown in Figures 1, 2, and 3. On the other hand this disentanglement is not a completely irreversible process, since it is known that, after removal of the applied strain, the sample will recover completely. This merely proves that the adhesion is strong enough to cause the chains to re-entangle, but not necessarily in their original configurations, so that chemical linkages play a secondary role relative to failure processes in highly filled composites.

Accepting the picture that chains will disentangle and yield, and will flow slowly under the retardation by particle-binder frictional forces, one is forced to conclude that the particles as well will tend to move to new positions of equilibrium while the stress is relaxing. One would like to know what sort of forces act on the particles. In our studies at GALCIT, we have separated this question into two parts, one of which we will discuss here. That is, what are the forces operating between the unbound particles? The other part which deals with the filler-binder frictional forces will be discussed in a subsequent report.

For the studies which we shall discuss, we worked with high speed micropulverized ammonium perchlorate particles ca. 40 μ in diameter. This type of material will not lose weight after sitting in an oven for three hours at 250°F., and yet the particles are definitely sticky to the touch. Thus any surface moisture is chemically bound and the material must be classified as cohesive, in the sense that cohesion is promoted by intersurface chemical forces. The precise nature of these forces does not concern us.

In contrast to ammonium perchlorate particles, sand is a non-cohesive material. Both of these granular media can be characterized by the concepts of soil mechanics, but the application to a medium such as sand is much simpler. We shall thus discuss some of the ideas of granular mechanics which do apply to sand (12) and simultaneously indicate the modifications that need to be introduced to characterize ammonium perchlorate.

The basic idea of granular elasticity is that stress is transferred through a granular body by normal and shear forces operating at points of contact between more or less regularly packed particles. These points of contact are actually deformed into areas of contact; and, under the assumption that the radius of the area of contact is small with respect to the mean radius of curvature of the two particles at the point of contact, Hertzian mechanics prevails and predicts a non-linear stress-strain relation. Further discussion of this type of mechanics does not concern us. In fact, we shall treat the particles as rigid and inquire of the forces acting on them.

In addition to forces generated by surface tractions, there may also be cohesive forces. This is certainly the case for ammonium perchlorate particles, a measure of which is expressed by the statement that a cylindrical hole 1" in diameter by 4" in depth may be dug with sheer sides. If the cohesion were zero, the hole would necessarily be conical, the angle of the cone depending on the static angle of repose of the particles.

The basis of viscous response in a granular medium lies in the departure of the packing from a so-called perfectly dense structure. Thus in any granular medium the result of viscous response is an increase in density termed <u>compaction</u>. In postulating the existence of a perfectly dense structure, it is assumed that all particles are spheres of the same diameter. This is a reasonable assumption for many granular materials. The perfectly dense structure for uniform spheres is either face-centered cubic or hexagonal in symmetry. It will be assumed that the reader is familiar with the basic geometries of these structures*. Looseness in granular media may be promoted either by removing an occasional sphere from a close-packed structure, or by mixing islands of close- and loose-packed structures. An example of a loose-packed structure is a simple cubic one.

Before discussing the process of compaction, let us analyze the forces that must operate in order for a dense structure to flow. Knowing this, we then can make an estimate of the forces involved in causing a loose structure to become dense. In retarding the operation of these frictional forces by some sort of relaxation process, we can then arrive at a basis for viscoelasticity in granular media. Finally we shall demonstrate this experimentally, and compare its time scale with that observed in propellants.

We discuss first a cohesionless medium (face-centered cubic structure). In the unit cell of this cube, there are four spheres, eight octants, the center of curvature of each octant placed at each of the eight apices of the cube, and six hemispheres, the center of curvature of each hemisphere placed at the center of each of the six faces of the cube. All octants and hemispheres are turned inward so as to be in interior contact, their plane surfaces facing outward.

If a hydrostatic pressure σ_3 be applied to such an array of spheres, the force normal to each face of the unit cube will be $8R^2\sigma_3$, since the edge of the unit cube is $2\sqrt{2}\,R$, where R is the radius of a sphere. The resultant force normal to the surface of the hemisphere in the center of a given face of the unit cube is $4R^2\sigma_3$ since the total face exposes one circle (the plane surface of the hemisphere) and four quadrants (the plane surfaces of the solid octants). This force is reacted to by four equal forces at the four points of contact of the hemisphere with four of the five other hemispheres; it does not contact the fifth. Its contacts with the four octants are orthogonal to the direction of the force we are discussing, and since there are no tangential forces because the loading is hydrostatic these four contacts do not contribute a resultant to the reactant force. The angle of contact between each of the hemispheres is $(\pi/4)$ measured relative to the direction of the force on the given face, so that the contact force between each pair of hemispheres is

---

* Further information may be found in R. Scott's Soil Mechanics, Addison-Wesley (1962).

$$\frac{4R^2\sigma_3}{4\cos\frac{\pi}{4}} = \sqrt{2}\,R^2\sigma_3$$

Now consider a hexagonal plane in which a given sphere is surrounded by six spheres in-plane, three above, and three below, for a total of twelve. The three spheres above contribute a total force normal to the given hexagonal plane $3\sqrt{2/3}\,\sqrt{2}\,R^2\sigma_3 = 2\sqrt{3}\,R^2\sigma_3$ where $(\sqrt{2/3})$ is the direction cosine of each upper sphere with respect to the normal. Now suppose that, in addition to this normal force, a force D making angle β with the $\overline{y}$-axis, in the $\overline{y}$ - $\overline{z}$ plane is added to the force system, where $\overline{z}$ is the axis normal to the hexagonal plane, $\overline{y}$ is collinear with a row of spheres in the plane, and $\overline{x}$ of course is orthogonal to the other two axes. The extra force D will tend to lift one hexagonal layer out of the valleys and cause it to slide over the cols (saddle valleys) into the next set of valleys. A simple force balance shows the minimum force needed to cause slippage for an assumed friction constant f is given by:

$$\frac{D}{2\sqrt{3}\,R^2\sigma_3} = \frac{1}{R\cos\beta - \sin\beta} \tag{23}$$

where

$$k \equiv \frac{2(\sqrt{6} - f)}{\sqrt{3} + 4\sqrt{2}\,f} \tag{24}$$

This force in turn is produced by a deviator stress acting at an angle β on the hexagonal plane. Since the projected area of the unit hexagon is $6\sqrt{3}\,R^2 \sin\beta$, and since one sphere occupies 1/3 the unit hexagon area, the force is given by:

$$D = (\sigma_1 - \sigma_2)\,2\sqrt{3}\,R^2 \sin\beta \tag{25}$$

Thus the work done in moving the sphere from a valley to a saddle point is proportional to $(\sigma_1 - \sigma_3)$, whereas by (23), the minimum force necessary to initiate motion is proportional to σ_3 and some function of the friction constant. In the case of cohesive materials, the minimum force must include a constant term to overcome cohesion so that the work done includes an energy constant for the breaking of cohesion. Accordingly, we write for ammonium perchlorate spheres

$$\Delta W = A + B\,(\sigma_1 - \sigma_3) \tag{26}$$

where A and B will be adjusted to fit available data. Strictly speaking, we should express A and B as functions of β in an analogous fashion to what was done in leading up to (23); however, we shall present experimental data only for a given β, and will not press the analysis further.

It has already been pointed out that the time scale associated with stress relaxation in composite propellants is of the order of several months. In order to assess the time scale of frictional force relaxation among granular particles, a series of tests was carried out in which HSMP ammonium perchlorate particles packed in a 4" x 1" thin rubber cylinder were loaded up with a constant hydrostatic pressure and an initial deviator load which was allowed to relax. Figure 8 shows the relaxation curves obtained at a given constant initial displacement. The precise value of this displacement is unimportant because of the lack of definition of the state of compaction of the sample from test to test. As a result the dimensionless ratio of instantaneous stress to initial stress is plotted.

Now let us consider the nature of the processes which retard the relaxation of stress. Patently they are frictional processes; but at the molecular level, friction loses meaning. Instead it is suggested that the atoms in the contact area in jumping around with a quantum frequency kT/h, where $\underline{k}$ and $\underline{h}$ are Boltzmann's and Planck's constant, respectively. Eyring has shown that when an atom with such a frequency is urged by a local force to jump over a potential energy barrier, then the rate constant of this jump process is proportional to the hyperbolic sine of the local stress concentration.

In order to define the rate constant for the jump process, we must take account of the realities of the packing. Actually there are probably islands of various types of regularity, various degrees of looseness, and various states of orientation. This is empirically equivalent to saying there is a distribution of relaxation times. A typical distribution function which works well for composite propellants (13) is the Cole distribution which leads to the following expression for stress relaxation.

$$\frac{\sigma}{\sigma_0} = \frac{1}{1 + kt^n} \qquad (27)$$

where k is the rate constant. Fairly good straight-line plots of $\log(\sigma_0/\sigma - 1)$ are shown in Figure 9. The order of magnitude of the log-log slopes $\underline{n}$ is just that found for composite propellants. (14) There is however an irregular variation of the slope with the hydrostatic pressure σ_3. Because of the lack of definition of the state of compaction, analysis of this effect cannot be pursued. Furthermore, in order to correlate the rate constant with the hyperbolic sine of the stress deviator, it is necessary to determine the temperature dependence of the relaxation process since the proportionality constant (B) of equation (26) which multiplies the stress deviator should go as one over the absolute temperature. Without this information virtually any constant can be chosen to give a good straight-line relation between the rate constant and hyperbolic sine of the stress deviator work term. So the main conclusion we can draw from these relaxation experiments is that the distribution of relaxation times is similar to that observed in propellants but the time scale of relaxation is shorter by perhaps a factor of five. This latter estimate is based on the facts that the time to relax to 1% of initial stress is six months for composites, one month for granular media of the type we are discussing.

In addition to relaxation data, we also ran creep data, the main features of which are summarized in Figures 10, 11 and 12. In Figure 10 we note that a sample subjected to initial constant load of 15 pounds creeps much more rapidly during the first cycle than the same sample in subsequent cycles. Furthermore, when the load is varied from 15 pounds to 30 pounds on the same sample (Figure 11), the creep displacement is not changed significantly. If a fresh sample (Figure 12) is cycled under a 30 pound load, again the first cycle produces much more creep than subsequent cycles which lie in the same range of displacement as was obtained with the first sample. Thus the first reaction of granular media to load is to compact. Presumably it does this under a minimum value of the stress deviator as shown by equations (23) and (25), modified to account for cohesion. The secondary reaction is primarily elastic.

Now by inference we can extend this line of thinking to bound granules, or composite propellants. Because of the elastic constraints of the binder, the amount of compaction is limited in that particles are not completely free to move in the direction of producing a dense structure. Furthermore, the amount of looseness in composites is much lower than that of granular media. The average soil has a porosity of 35%. The ammonium perchlorate we studied had a porosity of 48%, whereas a completely dense structure has a porosity of 26%. In the propellant most of this porosity is filled up by binder, leaving only a few tenths of one per cent porosity. This does not mean however that particles cannot achieve better packing with change in porosity. Furthermore, as a sample is stretched, the reverse process can occur in which particles decompact and then, under the influence of local stresses in the binder, can rearrange to new packing. This latter process is facilitated by the dilatation of the composite which ensues with stretch (cf. equation 7 and discussion).

Because of the frictional constraints of the binder, the rates of compaction, decompaction, rearrangement of particles, and slippage of the binder are all slower than in a granular medium. In fact, in most non-cohesive granular media, the relaxation is so fast as to be practically non-observable after a few seconds. Since this slow relaxation of stress in propellants is of import in practically every application, we consider it most important to determine next the time scale of the slippage of binder around particles. It is planned to initiate work in this area during the next report period.

VI. CONCLUSION

As the result of the creep and relaxation studies on ammonium perchlorate particles, we are led to three important conclusions. First, the time scale associated with the relaxation of frictional forces between particles is not as long as that associated with forces between particles and binder.

Secondly, the particles can compact or decompact, making for tremendous changes in the shear properties of a propellant as a function of superimposed hydrostatic pressure. This dependence should show up in a Mohr-Coulomb failure trace and has indeed been verified by Surland,(15) Kruse,(16) Heller, (17) and Vernon (18).

Thirdly, since ca. 80% of the propellant micro-structure is statically indeterminate, a deformed structure can accommodate a relatively large strain and hold it while relaxing the stress to zero. This strain is indeed elastic, but the instantaneous stress associated with it is not. Only after ca. six months will the stress have relaxed to its equilibrium elastic value of a few tenths of a psi. This implies that the effective modulus of an unfilled composite (one from which the ammonium perchlorate has been leached out) is roughly a hundred times less than that of the filled composite; and this is exactly what one observes after removal of the perchlorate particles. The resultant binder is quite a soft "cheesy" material. This latter statement should be verified quantitatively and will be in a subsequent report period. For the present, we can observe however that the modulus of the 47 vol. % voided foam used by Ko (19) in his thesis studies has a value of 30 psi which is a good factor of ten less than the modulus of the same binder filled with AP.

As a result of the stress relaxation studies on the glass-filled binder, we conclude that there are three regions of characteristic behavior evinced by most composites. In Figure 6 the region of rapid rise corresponds to storage of dilatational strain energy in the binder and filler in proportions determined by their respective bulk moduli. In this region, the value of Poisson's ratio of the binder is close to one-half. The second region, on which dewetting occurs rapidly, is one in which both Poisson's ratio and shear modulus decrease in value while adhesion bonds are broken and voids formed around each particle. The third region is one in which a slow rearrangement of the filler particles occurs. This slippage of the particles is probably attended by rehealing of the bonds. This conclusion is evident from the fact that recovery takes as long as stress relaxation.

REFERENCES

1. Blatz, P. J.; Olsen, F. N.: Monthly Progress Reports to Polaris Division, 1954 - 1958.

2. Blatz, P. J.: Fracture Studies on Composite Solid Propellants, 18th Meeting Bulletin of JANAF Panel on Physical Properties of Solid Propellants, p. 17.

3. Blatz, P. J.: The Yield Surface in Principal Stress Space, 19th Meeting Bulletin of JANAF Panel on Physical Properties of Solid Propellants, p. 165.

4. Blatz, P. J.; O'Callaghan, T.: Application of Large Deformation Theory to the Determination of Stresses and Strains in Internally Pressurized Propellant Grains. Appendix to 20th Meeting Bulletin of JANAF Panel on Physical Properties of Solid Propellants.

5. Treloar, L.R.G.: Physics of Rubber Elasticity, Oxford University Press (1958).

6. Blatz, P. J.; Ko, W. L.; Zak, A. R.: Fundamental Studies Relating to the Mechanical Behavior of Solid Propellants, Rocket Grains and Rocket Motors.

GALCIT SM 61-15	California Institute of Technology	June 1961
GALCIT SM 61-19	California Institute of Technology	Oct. 1961
GALCIT SM 62-14	California Institute of Technology	Feb. 1962
GALCIT SM 62-23	California Institute of Technology	May 1962
GALCIT SM 62-27	California Institute of Technology	Nov. 1962
GALCIT SM 63-5	California Institute of Technology	Feb. 1963
GALCIT SM 63-17	California Institute of Technology	May 1963

7. Blatz, P. J.: *Application of Finite Elastic Theory to the Behavior of Rubberlike Materials - To appear in Rubber Chemistry and Technology Reviews, 1963*.

8. Noll, W.: *Arch. Rat. Mech. Anal.* *2*, 197 (1958).

9. Ko, W. L.: *Application of Finite Elastic Theory to the Behavior of Rubberlike Materials, Ph.D. Dissertation, California Institute of Technology, June 1963*.

10. Blatz, P. J.; Ko, W. L.: Application of Finite Elastic Theory to the Deformation of Rubbery Materials. *Transactions of the Society of Rheology*, Vol. *6*, p. 223, 1962.

11. Ibid, p. 241.

12. Scott, R.: *Soil Mechanics*, Addison-Wesley (1963).

13. Cole, R.: Dielectric Relaxation in Glycerin, *J. Chem. Phys.*, *18*, 1417 (1950).

14. Landel, R.: Dynamic Mechanical Properties of a Glass-Bead Filled Polyisobutylene Binder, *Trans. Soc. Rheo.* *2*, 253 (1958).

15. Surland, C. C.: Stress Measurements on Hydrostatically Stressed Materials, *Experimental Mechanics*, *2*, No. 4, 110, April 1962.

16. Kruse, R. B.: Failure Behavior of Composite Solid Propellants, *21st Meeting Bulletin of JANAF Phys. Prop. Panel of Solid Propellants*.

17. Heller, R. A.; Stoll, R. D.; Freudenthal, A.M.: Anelasti-Plastic Behavior of a Filled Elastomer, ONR Proj. #064-446, Columbia Univ. Report, June 1962.

18. Vernon, J.: Biaxial Tensile Failure of Composite Solid Propellants, *21st Meeting Bulletin of JANAF Phys. Prop. Panel of Solid Propellants*.

19. *op. cit.* Ref. 9.

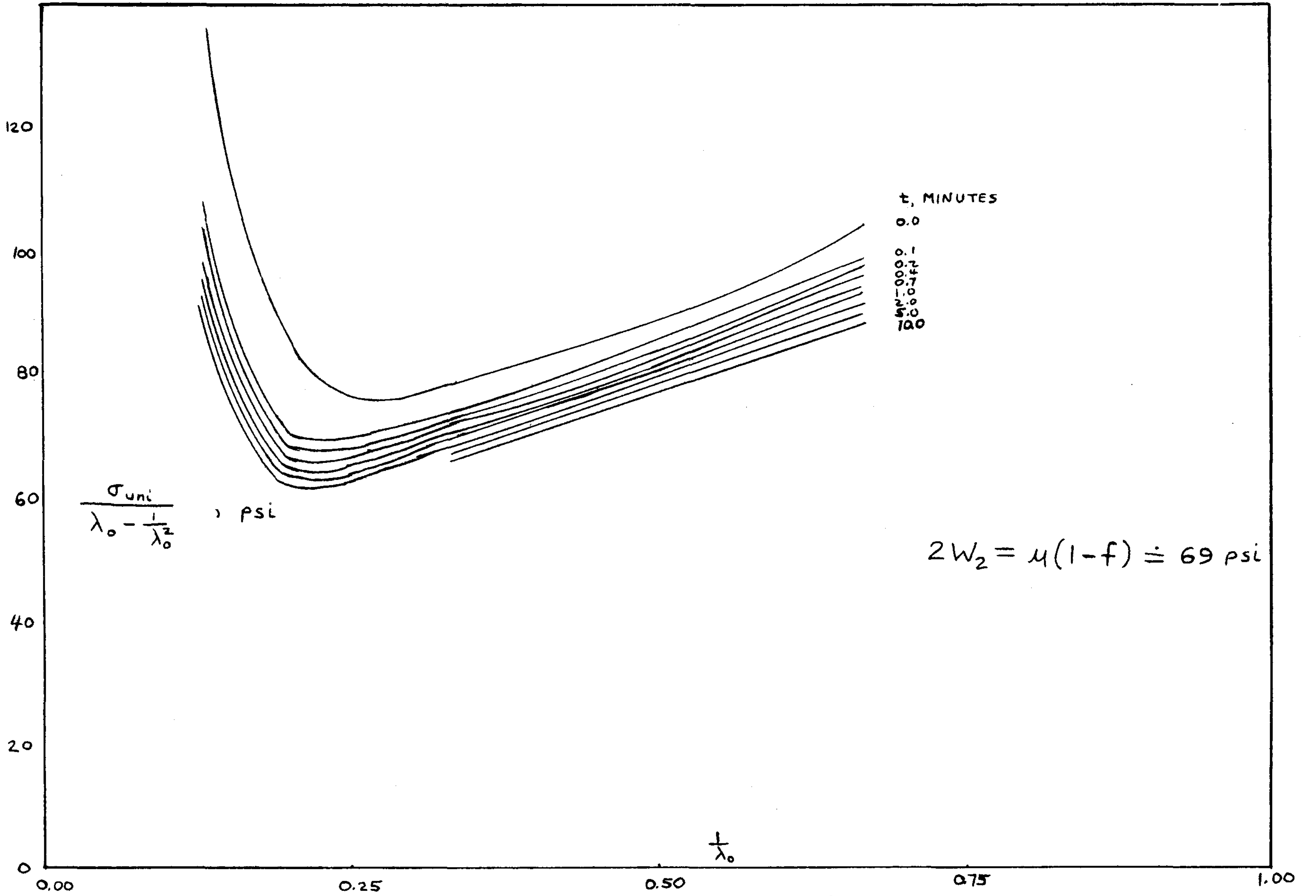

Figure 1. Stress Relaxation of Neoprene GNA at + 75° F.

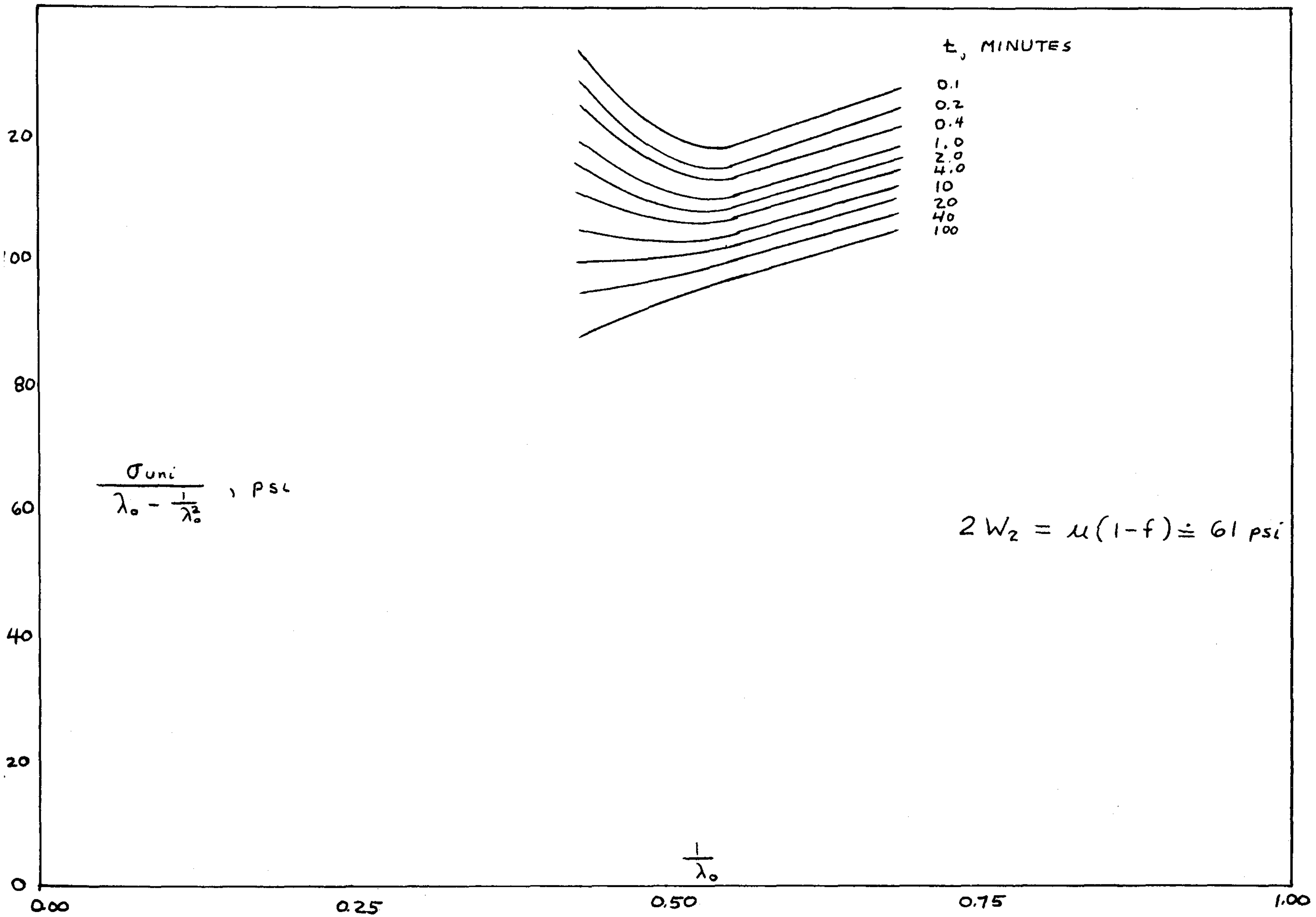

Figure 2. Stress Relaxation of Neoprene GNA at 0°F.

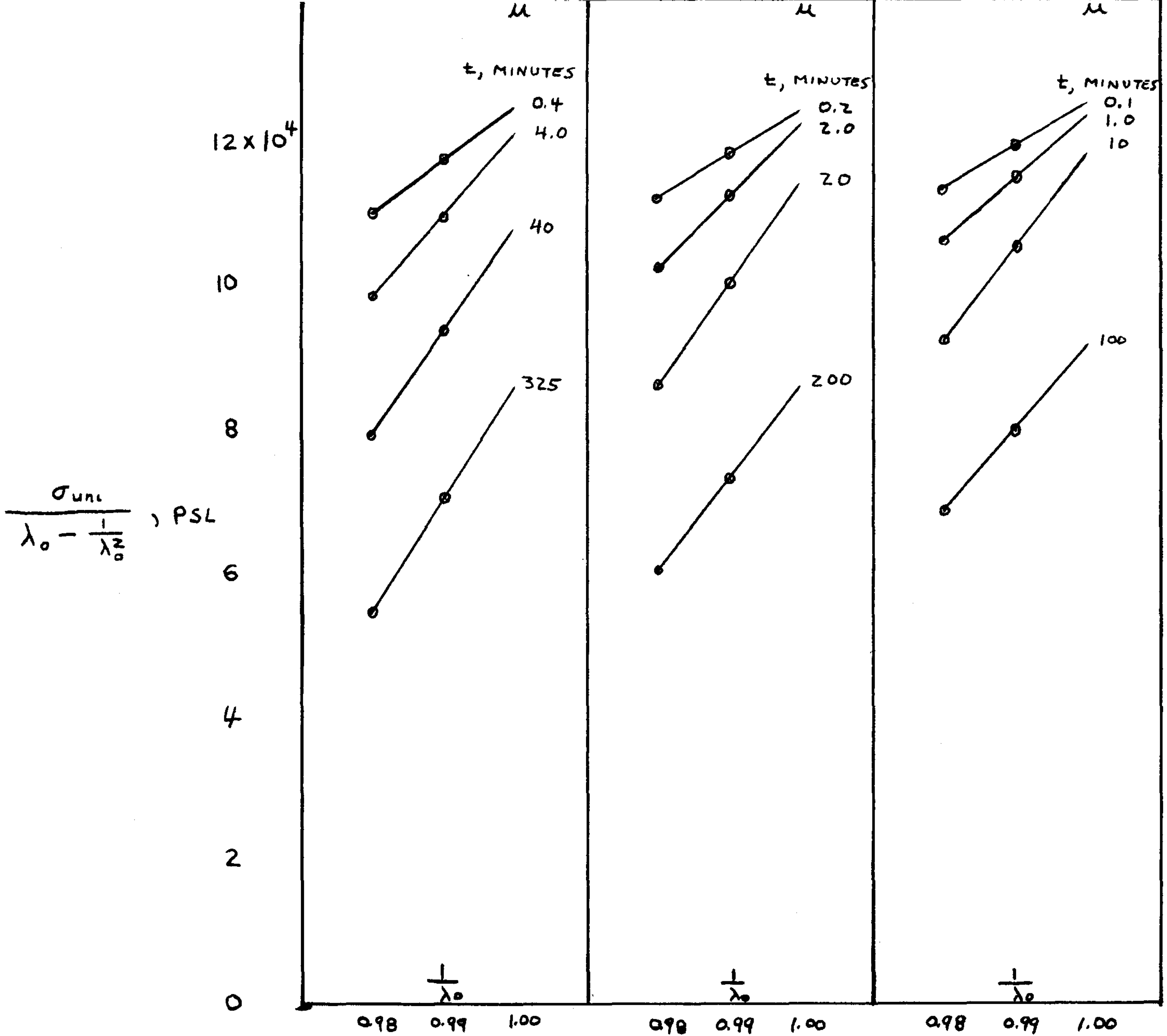

Figure 3. Stress Relaxation of Neoprene GNA at - 75°F.

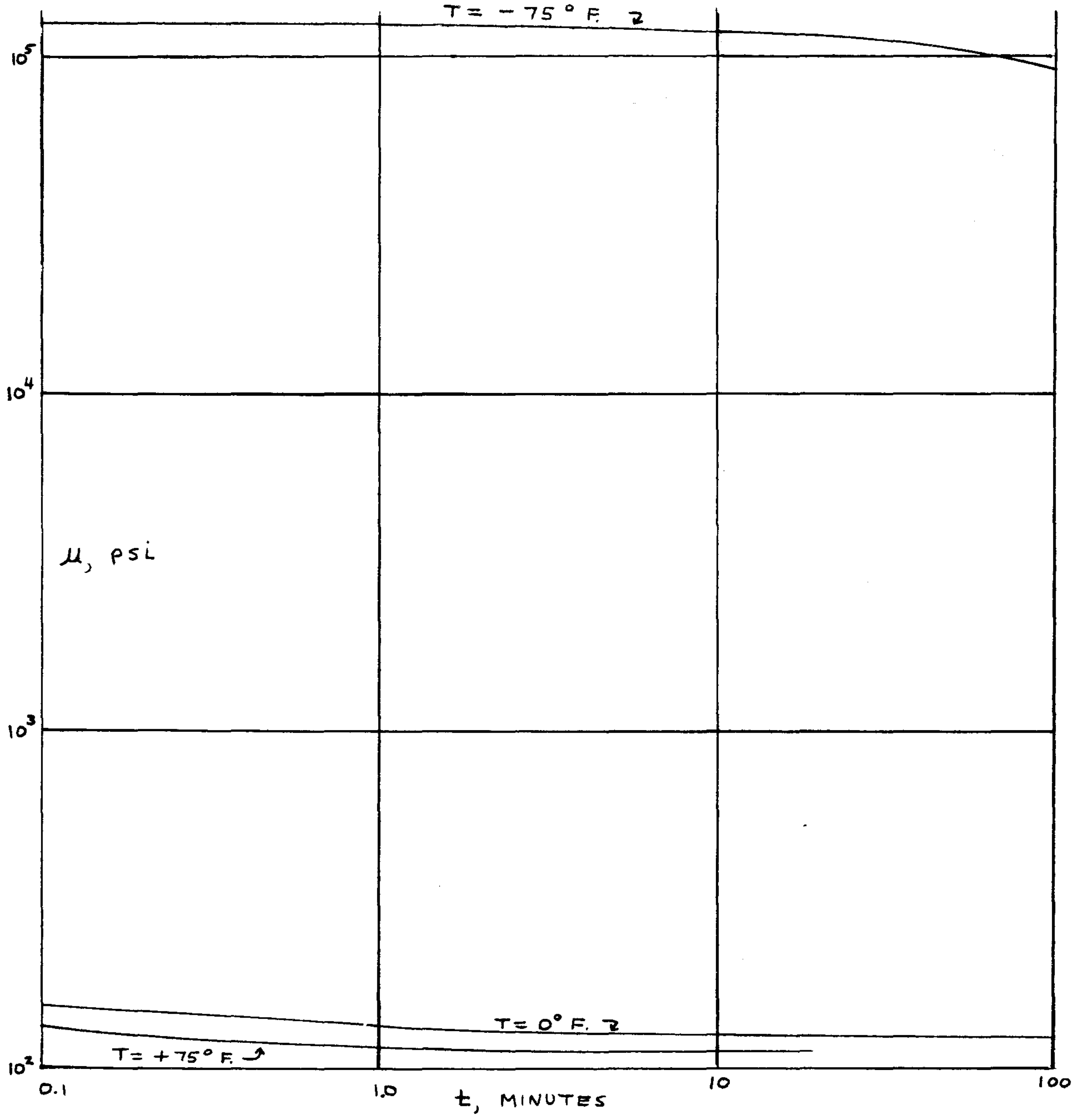

Figure 4. Time and Temperature Dependence of the Shear Modulus of Neoprene GNA

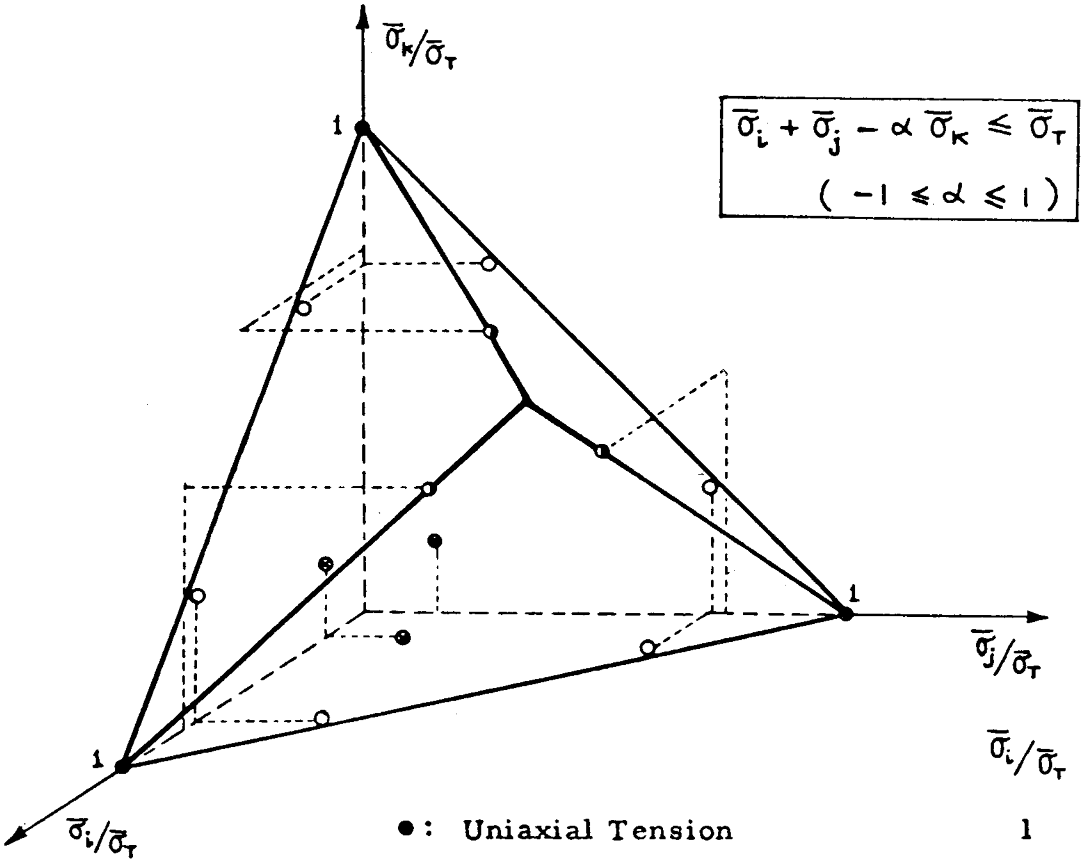

$$\bar{\sigma}_i + \bar{\sigma}_j - \alpha\,\bar{\sigma}_K \leq \bar{\sigma}_T$$
$$(-1 \leq \alpha \leq 1)$$

		$\bar{\sigma}_i/\bar{\sigma}_T$	$\bar{\sigma}_j/\bar{\sigma}_T$	$\bar{\sigma}_k/\bar{\sigma}_T$
●:	Uniaxial Tension	1	0	0
○:	Strip-Biaxial Tension	0.70	0.25	0
●:	Homogeneous-Biaxial Tension	0.15	0.15	0
◐:	Triaxial Tension	0.74	0.51	0.51

Figure 5. Plots of Experimental Failure Points in Principal True Stress Space (Polyurethane Rubber).

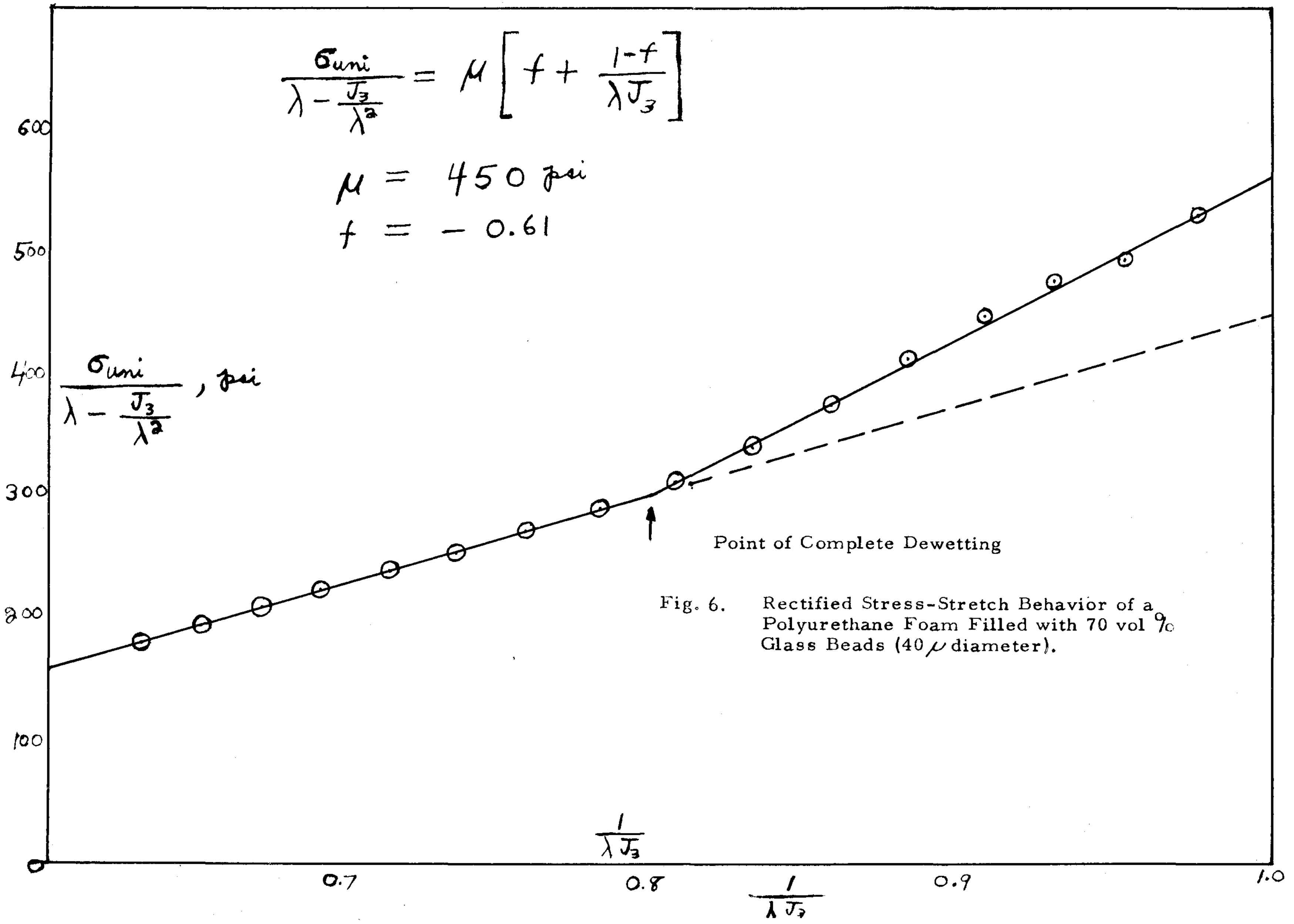

Fig. 6. Rectified Stress-Stretch Behavior of a Polyurethane Foam Filled with 70 vol % Glass Beads (40 μ diameter).

$$\frac{W_3}{\mu} = \frac{(1-f)\lambda}{J_3^2} - \frac{f}{\lambda}$$

$$\frac{W_3}{\mu} = \left[4(1-f) - \frac{2(1-\nu)}{1-2\nu}\right] + \left[\frac{1}{1-2\nu} - 2(1-f)\right] J_3$$

$$\nu \doteq \frac{1}{4}$$

Fig. 7. Dilatational Strain-Energy Gradient of a Filled Polyurethane Foam.

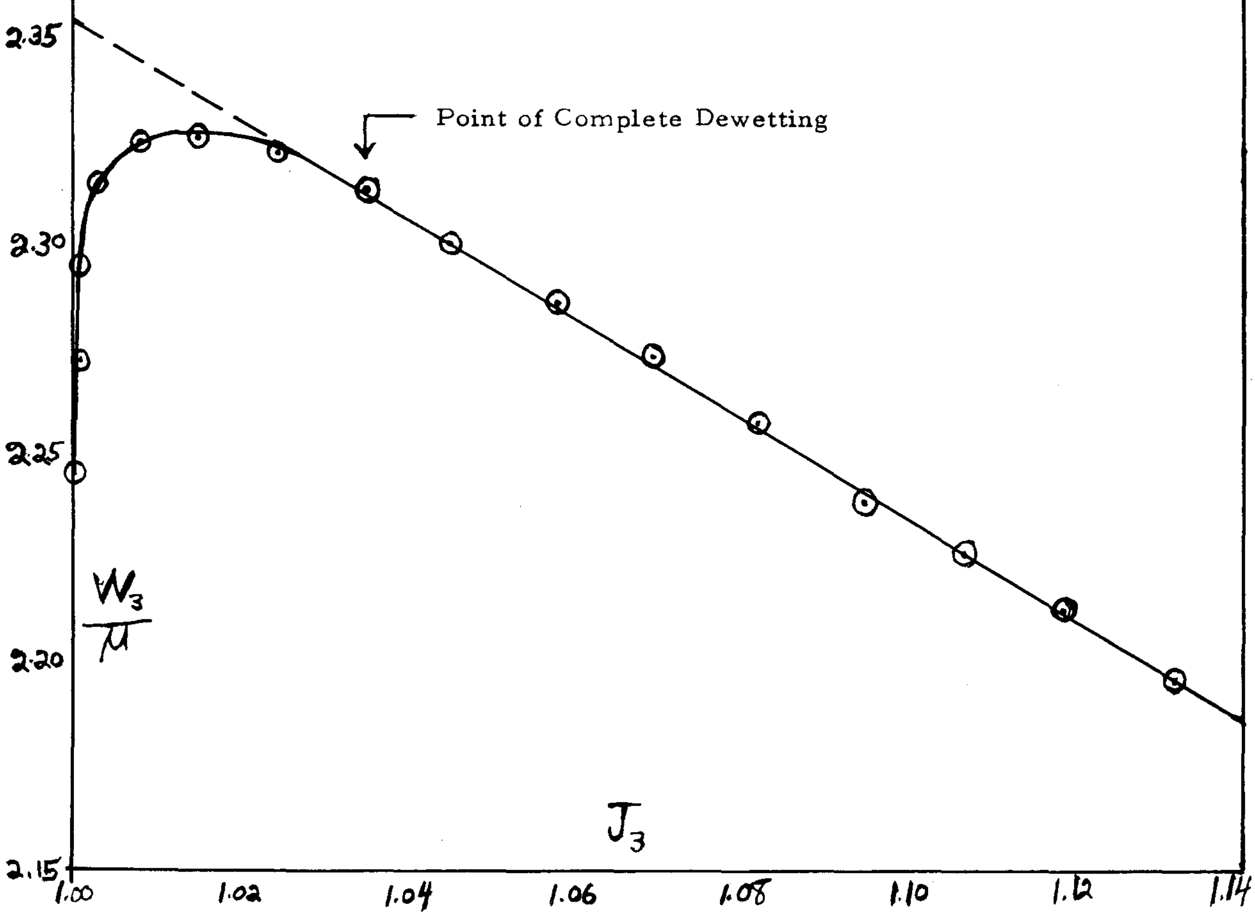

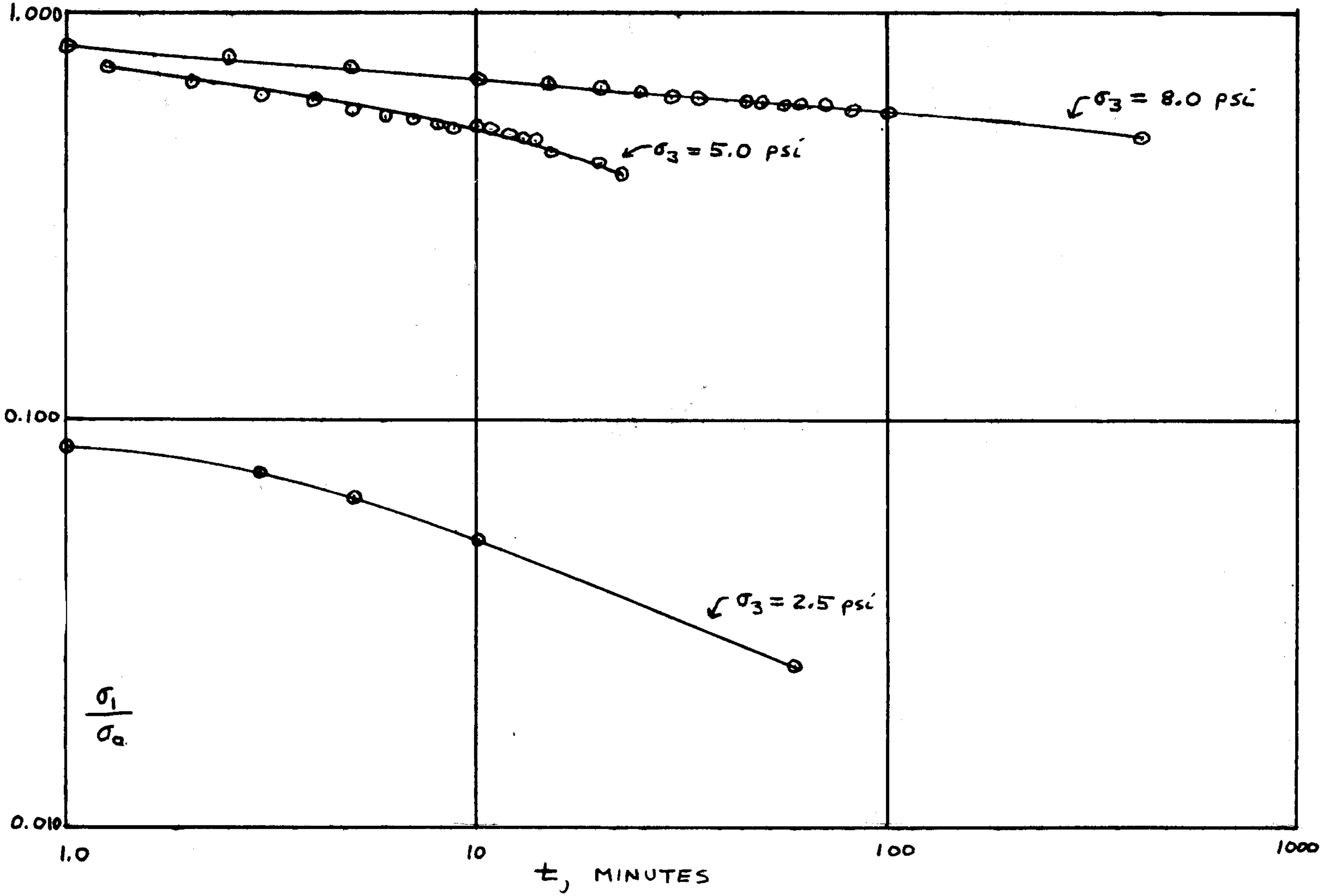

Figure 8. Stress Relaxation of HSMP-AP Particles (40 μ Diameter).

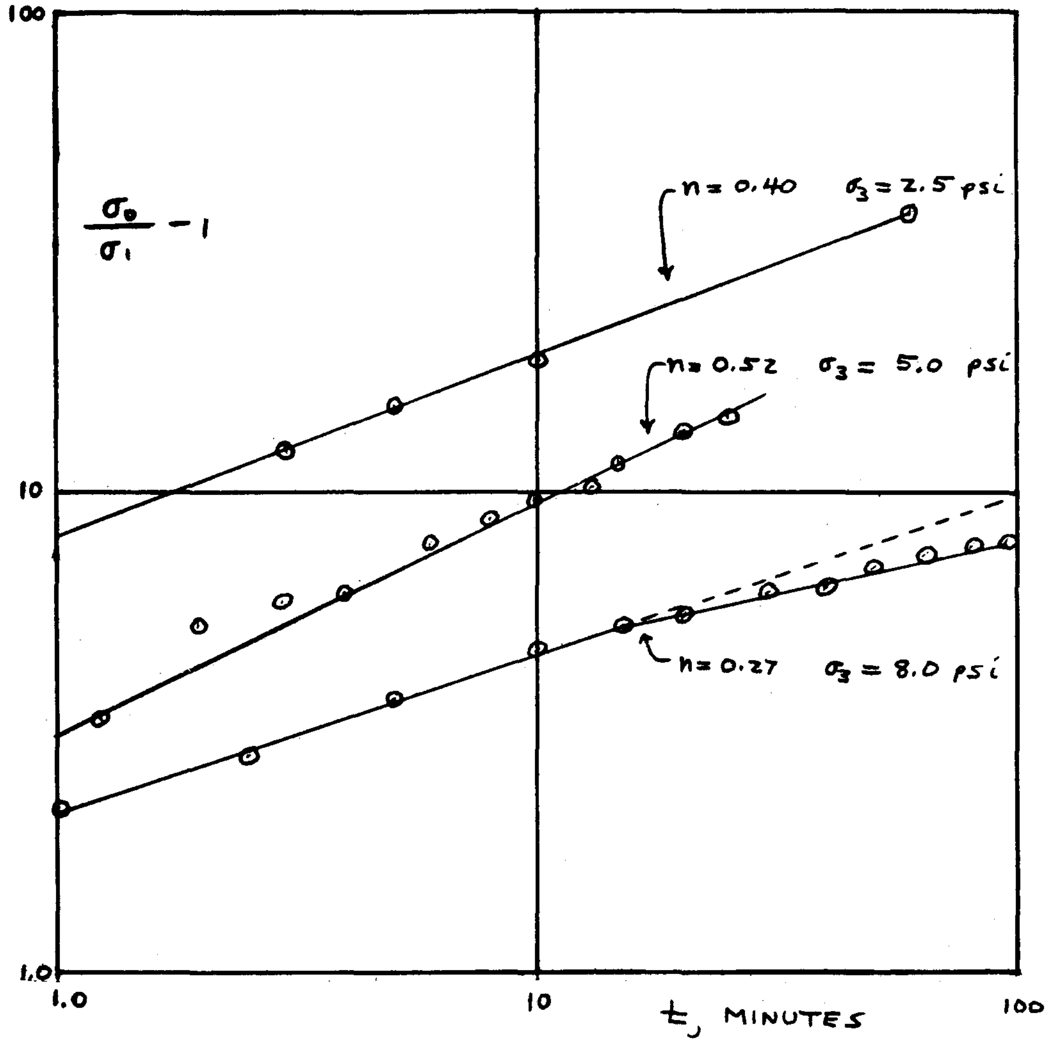

Figure 9. Stress Relaxation of AP Particles Rectified According to Cole Distribution Function.

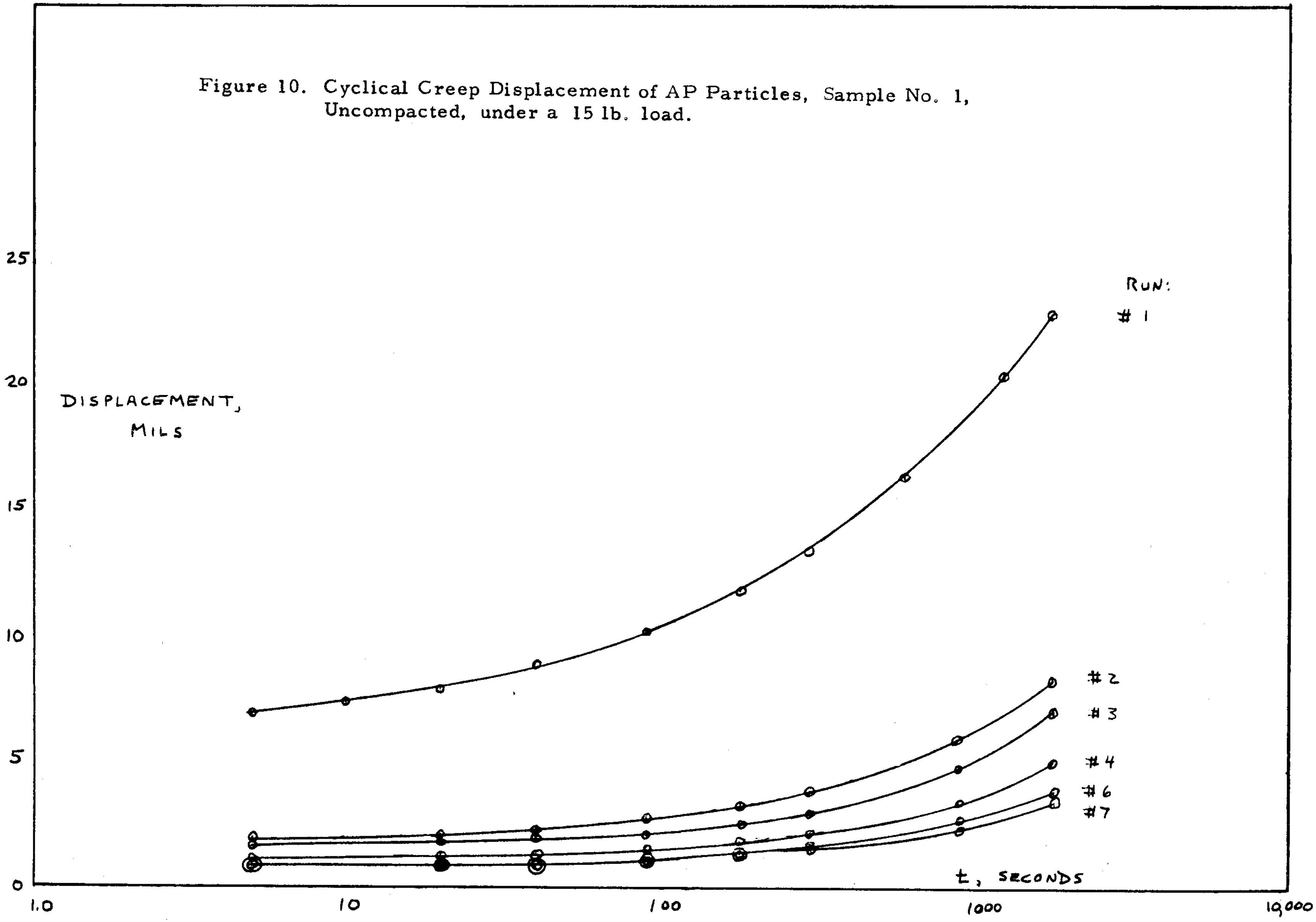

Figure 10. Cyclical Creep Displacement of AP Particles, Sample No. 1, Uncompacted, under a 15 lb. load.

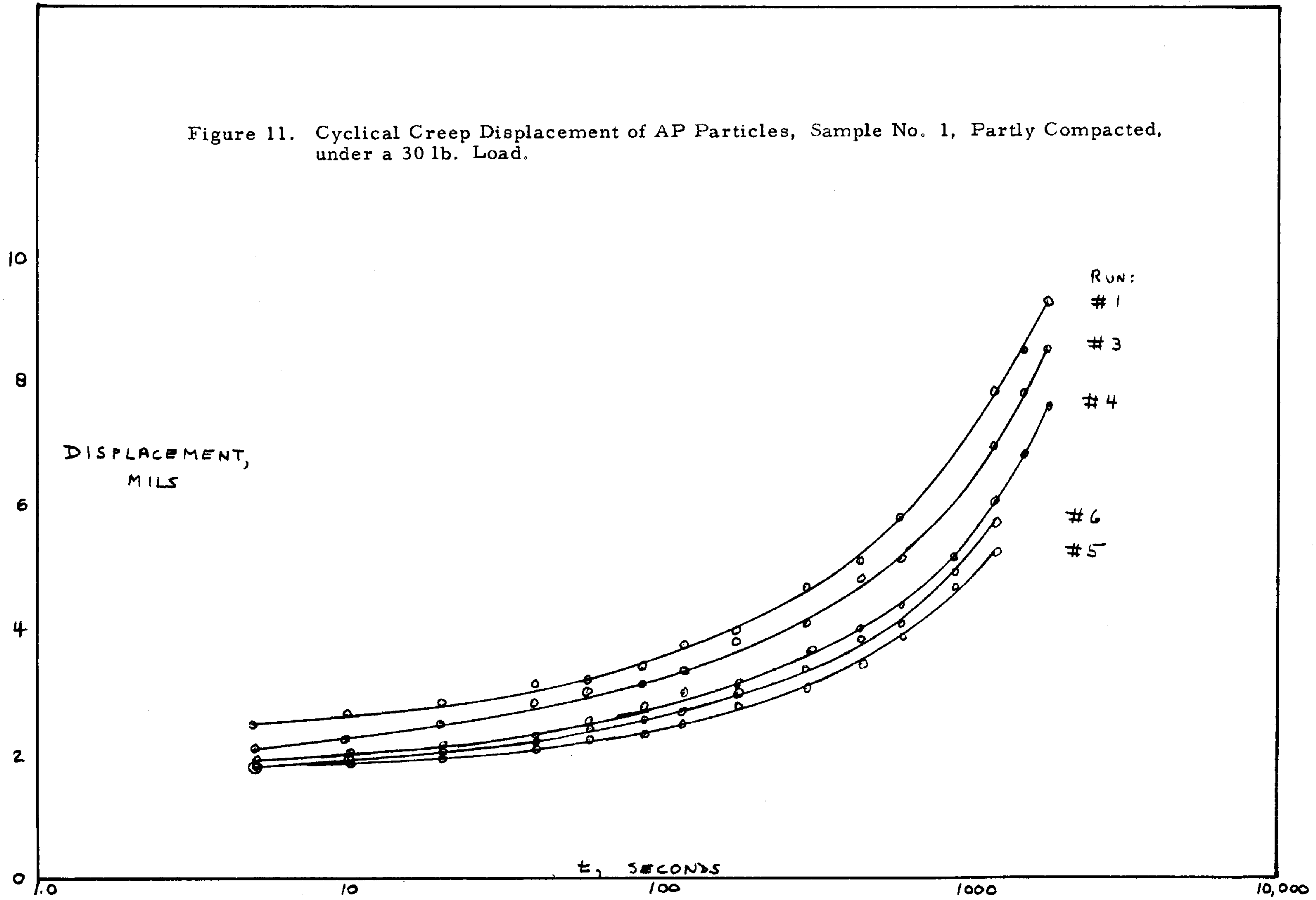

Figure 11. Cyclical Creep Displacement of AP Particles, Sample No. 1, Partly Compacted, under a 30 lb. Load.

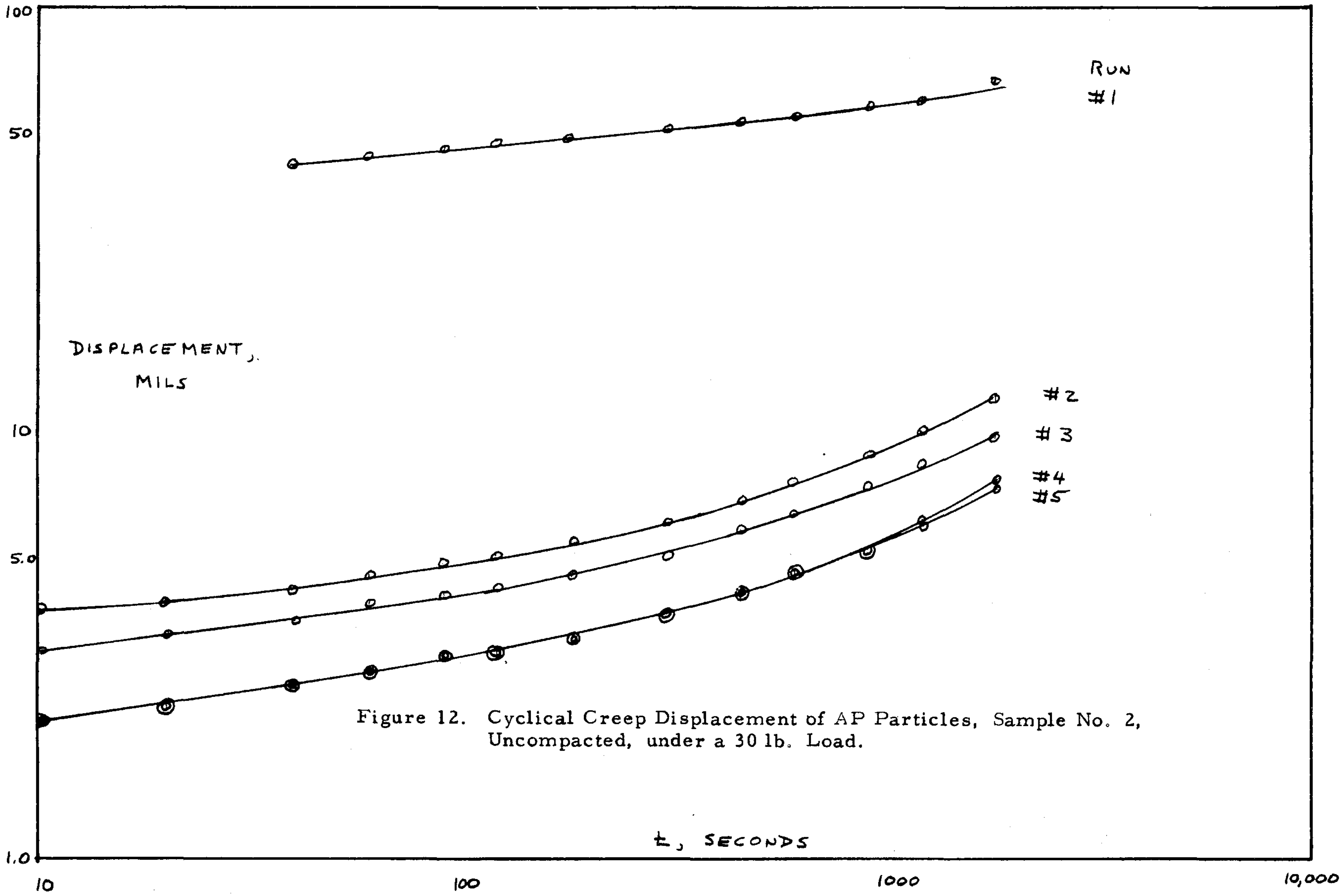

Figure 12. Cyclical Creep Displacement of AP Particles, Sample No. 2, Uncompacted, under a 30 lb. Load.